

# Biosynthesis and characterisation of zinc oxide nanoparticles from *Punica granatum* (pomegranate) juice extract and its application in thin films preparation by spin-coating method

Azeez Abdullah Barzinjy<sup>1,2</sup> ✉, Samir Mustafa Hamad<sup>3,4</sup>, Mahera Muhsin Esmaeel<sup>5</sup>, Semih Khurshid Aydin<sup>2</sup>, Faiq Hama Saeed Hussain<sup>6</sup>

<sup>1</sup>Department of Physics, College of Education, Salahaddin University-Erbil, Kurdistan Region, Iraq

<sup>2</sup>Department of Physics Education, Faculty of Education, Tishk International University, Erbil, Kurdistan Region, Iraq

<sup>3</sup>Scientific Research Centre, Soran University, Soran 44008, Erbil, Kurdistan Region, Iraq

<sup>4</sup>Computer Department, Cihan University-Erbil, Kurdistan Region, Iraq

<sup>5</sup>Department of Physics, College of Science, Salahaddin University-Erbil, Kurdistan Region, Iraq

<sup>6</sup>Department of Medical Analysis, Faculty of Science, Tishk International University, Erbil, Kurdistan Region, Iraq

✉ E-mail: azeez.azeez@su.edu.krd

Published in Micro & Nano Letters; Received on 13th August 2019; Revised on 23rd January 2020; Accepted on 19th February 2020

In this work, zinc oxide (ZnO) thin film has been assembled through the spin-coating method and accumulated on the p-type silicon (100) wafer. The ZnO nanoparticles (NPs) prepared via an entirely green procedure using *Punica granatum* (pomegranate) juice extract as an efficient chelating and capping agent. The coated ZnO NPs exhibited a homogeneous thin film over the silicon wafer. The crystal structure, surface morphology, alignment, and optical characteristics of ZnO thin film were studied through X-ray diffraction, field-emission scanning electron microscopy, EDX analysis, infrared spectroscopy, in addition to UV-vis spectra, correspondingly. The structure of the ZnO thin film was indexed as a wurtzite structure. UV-vis spectroscopy reveals that the alteration is straight bandgap energy ( $E_g$ ) and it is precisely 3.41 eV. The acquired ZnO thin films conceivably utilised as a photovoltaic material. The IR absorbance spectra indicate that the ZnO NPs spin-coated on the Si substrate improves the crystalline quality.

**1. Introduction:** Nanotechnology is a rapidly expanding zone of investigation, which possesses numerous uses cutting across numerous arenas. It is the procedure of governing matter at a very tiny level. This impression of employing matter at the nanoscale level led to a novel area of investigation and searched inside the scientific community which created an acceptable number of novelties and findings [1]. In nanotechnology science, a nanoparticle (NP) is well described as a tiny piece that acts by way of an entire component with regards to its transfer and characteristics. The discipline and manufacturing technology of nanosystems is accounted for as the greatest urgency as well as rapid growth areas of nanotechnology. It can be stated that each NP contains  $\sim 10^7$  atoms/molecules [2]. Current signs of progress in the nanotechnology field, mainly the aptitude to make highly well-organised NPs of whichever dimension and profile, have activated the improvement of its applications. Transition metal oxide nanostructure has attracted further arrangement of attention as a result of their exceptional physical and chemical characteristics emerging from big surface area/volume, quantum confinement consequence, that rely upon the outline and dimension of the substantial [3]. Between the numerous transition-metal-oxides, ZnO is a promising semiconductor substantial through wurtzite crystal construction take place as expected; nevertheless, it can be, generally, formed through chemical methods [4]. As a result of its exclusive characteristics, ZnO has been considered as a possible substantial for extensive choice of requests solely in transistors filed [5], colourant solar-cells [6], gas sensors [7], UV detectors [8], photocatalysis [9], biomedical uses [10] and thin-film transistors due to its extensive direct bandgap and sophisticated exciton binding energy at ambient temperature [11]. In addition, the technical impact of ZnO nanostructures, their pseudo-1D construction through the length in the limit of 10–100 nm, involved important attention from a technical viewpoint. ZnO fits into a retro of inorganic nanostructured fragments that are accessible by means

of an extensive choice of surface topography [12]. Particularly this bunch of metal oxides NPs is suitable for photo-catalysts and photo-oxidising aptitude in contrast to the biological and organic species [13].

The advantages of ZnO NPs over the other metal NPs are mainly caused by the height competence of UV obstruction, activation characteristics of the wide surface area as well as the exceptional uses in the cultivation area and biomedical sectors [14]. ZnO NP shows the antibacterial action counter to the microbial cells, as a result of the construction of hydrogen peroxide ( $H_2O_2$ ) otherwise stationary electric bonding of the subdivisions on the microbial surface [15]. There are diverse approaches that have been conveyed for producing ZnO NPs constructed by chemical and physical methods. Between these insufficient methods there are quite widespread approaches for producing ZnO NPs to build a thin film using the spin-coating method [3].

At present time biosynthesis, ZnO NPs is obtaining significance and has been suggested equally, like the promising process of physical and chemical approaches [16]. To adapt the structure, opto and magneto characteristics of ZnO NPs, it is important alterations to embellish the ZnO thin films through appropriate technique.

Overall, NPs are typically more toxic than the bulk material of larger scales [17]. Therefore, the green synthesis NP has been accomplished by means of ecologically adequate solvent schemes and eco-friendly reducing and capping agents. Conversely, the requisite for the biosynthesis of NPs rose since the physical and chemical methods are overpriced. Thus, in the exploration of a low-cost method for NP synthesis, researchers utilised bacteria and formerly plant extracts for the production of NPs. Natural surroundings have created numerous procedures for the production of nanoscale and microscale climbed inorganic ingredients which have been added to the growth of comparatively novel as well as a mainly uncultivated region of investigation built upon the green synthesis of nanomaterials [18].

*Punica granatum*, generally named pomegranate and belongs to the Lythraceae family [19]. Pomegranate juice has strong antioxidant, anti-inflammatory, antibacterial properties, the novel investigation has displayed some anticancer activities [20].

This investigation explored the synthesis of ZnO NP using pomegranate juice extract as a reducing agent. Then the synthesised ZnO NPs utilised as a thin film layer on the top of the p-type Si wafer. It can be stated that the ZnO NPs thin film can be utilised for many applications such as gas-sensing [21], UV emission LED apparatus [22], solar panel [23] and many others. The pomegranates collected from Halabja city (35.1655°N, 45.9896°E) in the Iraqi Kurdistan Region. According to our best knowledge, Iraqi Kurdistan is a supreme environment for growing pomegranates due to its middling temperatures, dry climate, i.e. possess the bottommost level of precipitation and moisture, and appropriate for farming. The best-known varieties originate from Halabja and Sharaban (in Diyala (33.7733°N, 45.1495°E)), both near the Iranian border [24].

## 2. Excremental part

**2.1. Biosynthesis of ZnO NPs:** As a sensitizer, pomegranate juice was prepared by the subsequent steps. Fresh seasonable red Halabja pomegranate seeds were crushed by means of a mortar, and the solid remainders were filtrated out. For the preparation of ZnO NPs, the pomegranate juice was utilised to make the aqueous extract. 50 ml of pomegranate juice extract syrup was added to 50 ml of zinc nitrate,  $Zn(NO_3)_2$ , (>1 M) dropwise under vigorous stirring at 80°C for 40 min, in addition, the pH of the mixture was controlled by adding NaOH till fluctuating the colour of the solution has been observed at pH 12, which is resulting in the surface plasmon resonance (SPR), as checked by UV-vis method, followed by the creation of some snowy sedimentation. In most circumstances, the interaction of plant phytochemicals with metal salts alter the colour of the reaction mixture as an indication of nanostructure formation resulting from the appearance of SPR signs as can be detected by means of UV-vis spectroscopy [25]. Indeed, this method effortlessly proves the formation of nanostructure as it is a thumbprint technique; in this case, the green synthesised NPs display their SPR sign in a resolute range. Thus, the pink coloured solution turned white slowly, indicating the formation of ZnO NPs. The sedimentation was totally separate by using centrifugation at 7500 rpm and acquired powder cleaned with methanol and deionised water several times to remove possible sedimentation. Finally, simulated-annealing followed out on the Bunsen burner flame at ~500°C for ~1 h, as shown in Fig. 1.

X-ray diffraction (XRD) experiments were implemented by means of a PAnalyticalX' Pert PRO (Cu  $K\alpha = 1.5406 \text{ \AA}$ ). The scanning rate was 1°/min in the  $2\theta$  range from 20° to 80°. UV-vis spectroscopy investigation was verified on a double beam spectrophotometer (Super Aquarius spectrophotometer) to certify the production of ZnO NPs. Morphology and particle spreading were studied through field emission scanning electron microscopy (FESEM) (Quanta 4500). The chemical configuration of the arranged nanostructures was studied by EDX (energy-dispersive X-ray spectroscopy) implemented a FESEM. FTIR study was

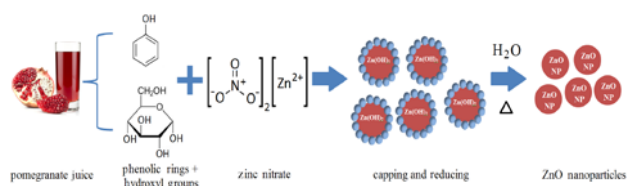


**Fig. 1** Possible mechanism for the formation of ZnO NPs using pomegranate juice

supported by a Perkin Elmer FTIR spectrophotometer through a resolution of  $4 \text{ cm}^{-1}$ .

**2.2. ZnO thin films synthesis:** As presented in Fig. 2, only 2 mg of ZnO NPs, prepared as mentioned previously, was mixed with 20 ml of the methanol and magnetically stirred at 50°C for 2 h until the mixture becomes a totally colourless solution. The finishing mixture was utilised as a coating solvent. The p-silicon wafer substrate was washed in acetone and methanol by using an ultrasonic bath cleaner. Then the substrates were washed with double distilled water and then dehydrated at ambient temperature. The dried substrate was stabilised on the spin coater disk. A 1 ml of precursor solvent was added to the Si substrate by injection at 3000 rpm for half a minute. Afterwards, the deposited film was dehydrated at 150°C for 2 min on the hot plate in order to eliminate any left behind ingredients. This procedure was carried out at room temperature. Also, the deposition and dehydrating procedure were performed four rounds up to the achievement of the optimal thickness. Finally, the prepared films were annealed at 400°C for 15 min in the oven to achieve an extremely crystalline ZnO thin film. The annealing process creates enhanced physical supplement which develops the electronic connection among entire particles of the thin films; then, the thin films were experienced gentle cooling at ambient temperature. The morphology of the ZnO thin film and its compositions were detected by a FESEM. The structures of ZnO film were described by PAnalytical-XRD. XRD is utilised to classify the crystallinity and segments of the ZnO film. The measurements were acquired at  $2\theta$  degrees using Cu  $K\alpha$  emission.

**3. Results and discussion:** The possible mechanism for the formation of the biosynthesised ZnO NPs using pomegranate juice extract can be shown in Fig. 1. The main class of pomegranate phytochemicals is the polyphenols (phenolic rings with multiple hydroxyl groups) that are plentiful in the fruit. The phenolic rings and multiple hydroxyl groups can react with  $Zn^{+2}$  to form the complex molecules of  $Zn(OH)_2$  through the capping and reducing processes. During annealing treatment, the complex turn into ZnO NPs [26].

The existence of polyphenolic compounds and the preparation of NPs can be proven through UV-vis and FTIR spectra of plant extract and acquired NPs. The absorbance spectrum of the prepared pomegranate juice is shown in Fig. 3. The specified bands of pomegranate juice were observed at 260 nm (bond I) and 363 nm (bond II). The main class of pomegranate phytochemicals is the polyphenols (phenolic rings with multiple hydroxyl groups) that are plentiful in the fruit. Pomegranate polyphenols contain flavonoids (flavonols and anthocyanins), condensed tannins (proanthocyanidins) and hydrolysable tannins (ellagitannins and gallotannins) [27]. According to the authors' best knowledge, the appearance of the peak, with 363 nm, in the diluted pomegranate juice is due to the existence of 0.35 mg of zinc per 100 g of pomegranate juice [28]. Thus, the ZnO NPs peak in Fig. 4 is very close to this peak.

The pomegranate juice extract is recognised to possess entire phenolic compounds, which offer high antioxidant potential. The efficient groups existing in the pomegranate juice extract and

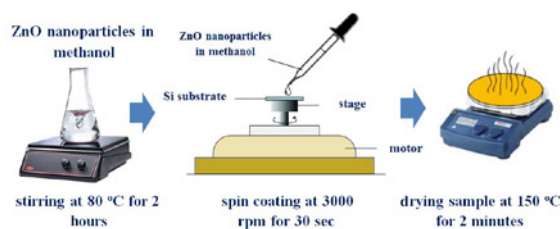


**Fig. 2** Preparation steps of ZnO NPs thin films by a spin coating method

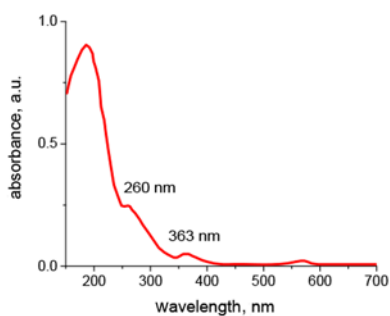


Fig. 3 UV-vis spectrum of diluted pomegranate juice in water 200:1

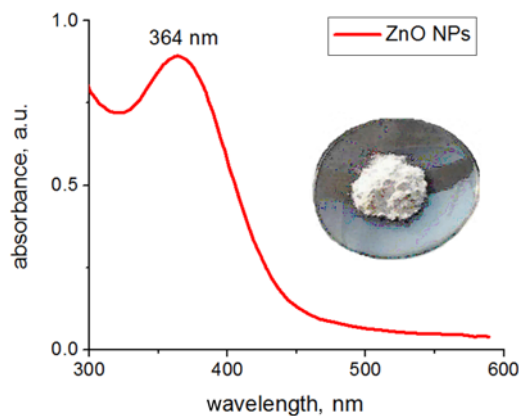


Fig. 4 UV-vis spectrum of the synthesised ZnO NPs

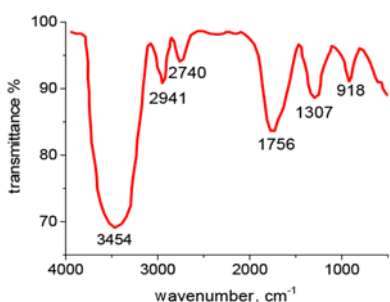
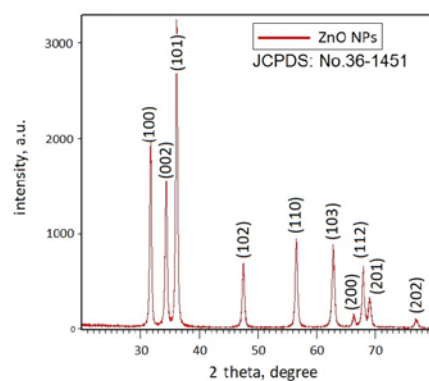


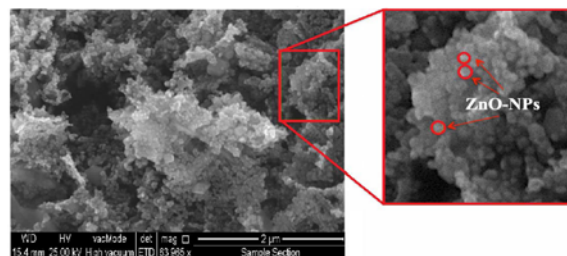
Fig. 5 FTIR spectrum for the pomegranate juice extract

ZnO NPs were investigated by means of FTIR spectroscopy. Based on the FTIR analyses presented in Fig. 5, the dominant peaks are 3454, 2941, 2740, 1756, 1307 and 918  $\text{cm}^{-1}$ , which were close to those of polyphenols specified by Nisha *et al.* [29]. The absorption peaks located at 3454 as well as 2941  $\text{cm}^{-1}$  specifies the existence of O–H stretching vibrations of phenolic group and C–H stretching of fatty acid chain compound, respectively. While the sharp characteristic peak at 1756  $\text{cm}^{-1}$  is related to the C=O stretching absorption. However, the most important peak is a very wide-ranging peak at 3454  $\text{cm}^{-1}$  due to the hydrogen bonding interaction of polyphenols –OH groups existing in the extraction. The OH biomolecules causative for the reduction of ZnO and capping agent of bio-reduced ZnO NPs over certain vibration bonds peaks approaching at distinct wavenumbers.

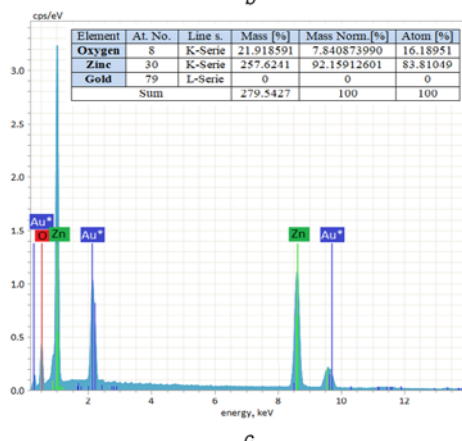
Accomplished ZnO NPs were described by XRD, SEM and EDX exploration, which are presented in Fig. 6. The XRD pattern of ZnO NPs synthesised by the biological method presented in Fig. 6a and it shows the hexagonal wurtzite arrangement. As of the XRD pattern, the governing reflection planes were (100), (002), (101), (102), (110), (103), (200), (112), (201) and (202)



a



b



c

Fig. 6 Crystal structure, morphology and elemental analysis of biosynthesised ZnO NPs prepared from pomegranate juice

a XRD  
b SEM (with magnification)  
c EDAX analysis

associated with scattering angles 32°, 34°, 36°, 48°, 57°, 63°, 66°, 68°, 69° and 77° correspondingly. The acquired peaks counterparts with the JCPDS Card No. 36-1451 specifies that the ZnO is an unadulterated crystalline having hexagonal wurtzite structure [30]. Moreover, the improved and close-fitting scattering peaks are acceptable signs to verify the pureness and crystallinity of the prepared ZnO NPs from this investigation. From the dominant diffraction peak, associated with the plane (101), using Scherrer's equation, one can find the typical crystalline dimension of the ZnO NPs which is nearly 60 nm. Senthilkumar *et al.* utilising leaf aqueous extraction of *Tectona grandis* as the reducing agent and zinc nitrate as the precursor found similar results to this study [31].

It can be understood from Fig. 6b that the synthesised ZnO NPs were delineated as a consistent, combination, and separable from possessing any additional dominant appearance. Overall, the ZnO NPs are ball-shaped, and the dimension of the particle was nearly 50 nm as average, which is analogous to our earlier reckoning utilising Scherrer's equation.

Fig. 6c represents the EDX analysis, which is basically the distribution of only two components, oxygen and zinc, in the prepared

ZnO NPs. The presence of gold is as a result of the sample coating throughout SEM imaging. The distributions of these two components are ordered through the spreading of ZnO NPs. It can be noted that from an inset table in Fig. 6c, the accumulation of oxygen is nearly 16%, which is basically lesser than the concentration of zinc, about 84%. Also, the amount of zinc in the ingredient spreading of ZnO NPs is more than that of the representing outcomes by Senthilkumar *et al.* [31]. Although the content of oxygen is fewer than zinc, it homogeneously distributed on the surface of ZnO NPs.

The optical properties of biosynthesised ZnO NPs were inspected through UV-vis spectroscopy, as shown in Fig. 4. The observed peak at 364 nm supports the formation of ZnO NPs utilising green process [32].

Characteristically, NPs own a wavelength beneath the censorious wavelength of light. This makes them clear as crystal, a characteristic that marks them extremely suitable for requests in powder and paint, coverings, and packing. Moreover, the absorption peak at 364 nm related to the essential bandgap energy of the ZnO structure due to the electron movement from the valence band to the conduction band [33]. In this Letter, the bandgap energy of ZnO was equaled to 3.41 eV. Similar results have been obtained in [34]. The obtained result, i.e. bandgap  $\sim 3.41$  eV, is considerably blue-shifted once associated with the absorption inception of the bulk ZnO (370 nm and 3.35 eV) at ambient temperature [35]. Singh *et al.* using Madar (*Calotropis procera*) plant for preparation ZnO NPs found comparable results [36]. This upsurge in bandgap energy, allied with reducing particle dimension, is demonstrated using a blue-shifted in absorbance and photoluminescence study. ZnO NPs, normally, possess an extensive bandgap ( $\sim 3.4$  eV) and enormous exciton binding-energy (60 meV) and therefore is anticipated a best-talented nominee for nanooptoelectronics, sensing devices, transistors, nano piezo-electronics and UV-region detectors [37]. Explicitly, when the particle dimension is reduced, blue-shift might happen and therefore decrease UV protecting effectiveness [38]. A numeral of investigations has concentrated on classifying the critical size, which is necessary to attain high UV protecting effectiveness. For instance, Li *et al.* [39] manufactured diverse ZnO NPs through the calcination of the ZnO pioneer at diverse temperatures and combined them into epoxy resin. They acquired optimum optical characteristics in respect of shielding effectiveness.

Fig. 7 illustrates the XRD pattern of green synthesised ZnO thin film on the P-Si substrate, and it agrees with the hexagonal-wurtzite structure (Fig. 8). Here, we have settled solution-processed semiconductor oxide transparent thin film using the spin coating method. In general, transparent thin-film devices utilising polycrystalline ZnO as an active layer have been described to possess mobility values around  $0.2\text{--}2\text{ cm}^2\text{ V/s}$  [40].

Among many substrates, Si is the utmost widespread substrate as a result of its low-priced, extraordinary crystallinity precision, and

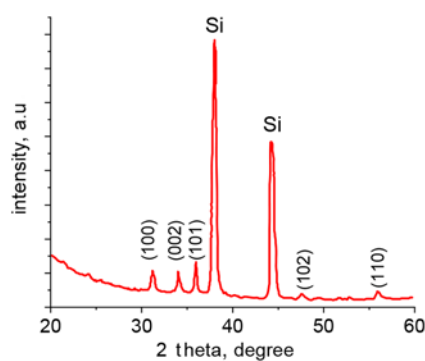


Fig. 7 XRD configuration of ZnO thin film grown on the Si substrate

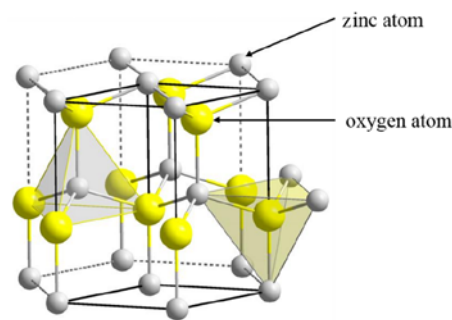


Fig. 8 Hexagonal wurtzite structure of ZnO [41]

high efficiency in large area wafer [42]. From the XRD pattern the governing reflection planes are (100), (002), (101), (102), (110), and two sharp Si peaks which corresponding with the scattering angles at  $31.6^\circ$ ,  $34.3^\circ$ ,  $36.3^\circ$ ,  $47.5^\circ$ ,  $56.5^\circ$ , and for p-Si substrate at  $38.2^\circ$  and  $44.1^\circ$ , respectively. The polycrystalline attribute hexagonal construction of ZnO is presented via (101) standard orientation at  $2\theta = 36.3^\circ$ . Likewise, short intensity peaks are presented via (100), (101), (102), (110), and (103) lattice alignments, as displayed in Fig. 7. It can be also noted, from Fig. 7, that the diffraction intensity from the (100), (002) and (101) planes is relatively stronger in contrast with that of the former chief planes, e.g. (102) and (110). In a similar attempt Wei *et al.* obtained ZnO nanocolumnar thin film on Si (111) wafer using pulsed laser plating [43]. They stated that the (101) plane is related to the hexagonal ZnO with a wurtzite construction; however a favourite orientation lengthways with the (002) plane is stronger.

The acquired peaks counterparts via the JCPDS Card No. 36-1451 specifies that the ZnO is an uncontaminated crystalline taking hexagonal-wurtzite structure [30]. The crystalline length can be easily calculated through Scherrer's equation,  $D = (0.94\lambda) / (\beta \cos\theta)$ , where  $D$  is the crystalline length,  $\lambda$  is the X-ray wavelength, equals to  $1.5406 \text{ \AA}$ ,  $\beta$  is the full-width half-maximum (FWHM) of the peak (101),  $\sim 0.003$ , from the Origin Pro9. Thus, the typical crystalline dimension of the ZnO structure based on  $D = (0.94\lambda) / (\beta \cos\theta)$  is 60 nm. Definitely, no additional peaks are perceived, and this points out that pure ZnO structure has been formed on the substrate. Generally, the pH value, category of extracts, aging-time and post-heat management are significant parameters that control the nature and dimension of part and parcel of NPs being produced [44].

The surface morphology and features of the deposited ZnO thin film on the Si wafer are depicted in Fig. 9. In general, small and even grains are dispersed on the ZnO NPs surface for the thin film grown on p-Si (100) wafer. In this research, it can be noticed from the FESEM graph (Fig. 9a) that indistinguishable distribution and to a certain degree ZnO NPs are rounded in shape. The

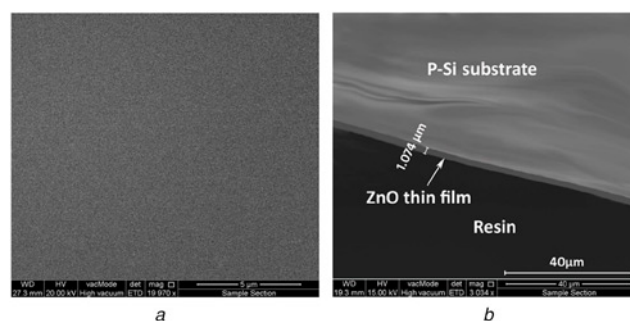


Fig. 9 Morphological characterization of ZnO NPs thin film on Si wafer  
a Thin-film morphology  
b Thin-film thickness of ZnO NPs deposited on the Si wafer

thickness of the thin film is also calculated through SEM images (Fig. 9b) and it was  $\sim 1 \mu\text{m}$ . The dimension of the particle was roughly 55 nm, which is equivalent to our XRD measurements utilising Scherrer's equation.

Fig. 10 represents the EDX investigation of ZnO thin film, which is prepared by means of green reduction procedure. The EDX analysis verified the presence of the zinc as well as oxygen on the top of the p-Si wafer. The existence of the Zn and O peaks characterised the fundamental description of the ZnO nanostructure. From the associated table in Fig. 10 regarding the EDX analysis, the weight percentages of Zn and O were 35.15 and 23.65%, correspondingly. While, the atomic percentages of Zn and O were 20.79 and 19.90%, respectively, and the residual, i.e. 59.30%, goes for the Si substrate. Therefore, it can be stated that the atomic fraction of Zn/O is bigger than one and the thin film stoichiometry will not change throughout the sputtering with the oxygen flux. Also, increasing oxygen flow causes decreasing in the deposition rate, which in turn influences the film crystallinity.

Together with the EDX, XRD as well as SEM micrographs, one can admire that ZnO NPs were exactly formed by means of the biosynthesised method.

The IR absorbance spectrum of ZnO/p-Si(100) films deposited at room temperature is given in Fig. 11.

The absorption band at a wavenumber of  $611 \text{ cm}^{-1}$  is a local vibration of substitutional carbon in a Si crystal lattice [41, 45]. In Fig. 11, the spectrum contains three absorption bands at

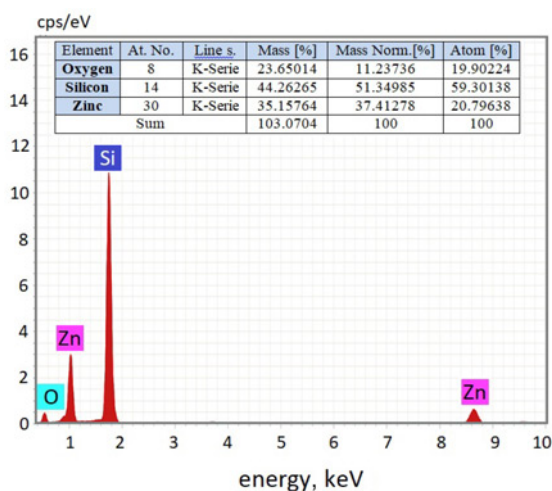


Fig. 10 EDX analysis of green synthesised ZnO thin film by using the extract from pomegranate juice

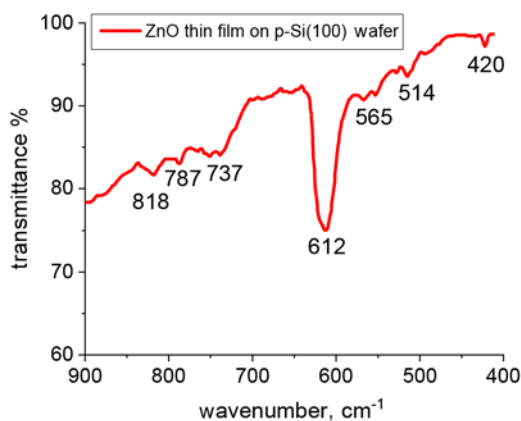


Fig. 11 FTIR spectra of ZnO thin film deposited on p-Si(100) substrate

wavenumbers  $420$ ,  $514$  and  $565 \text{ cm}^{-1}$ , respectively. The band located at  $420 \text{ cm}^{-1}$  is a typical ZnO absorption attributed to the bending vibration absorption of Zn–O bond, which corresponds to the  $E1$  symmetry transverse optical phonon mode, and the absorption intensity is increased obviously [46]. While both  $514$  and  $565 \text{ cm}^{-1}$  peaks include those for the crystal (lattice) and coordinated water. The formation of water is a consequence of the reaction of ZnO NP with a methanolic medium [47]. The reason for that should be the ZnO thin film deposited on the Si substrate presents merely the  $c$ -axis orientation growth. The observation of IR absorbance spectra shows that the ZnO thin film fabricated on the p-Si substrate improves the crystalline quality.

**4. Conclusion:** *Punica granatum* (pomegranate) juice extract contains polyphenolic biomolecules, can be used as reducing and capping agents for producing ZnO NPs in a green, one-pot and low-cost process. The biosynthesised ZnO NPs have been characterised using different characterisation methods. Then, the ZnO NPs have been dissolved in methanol and a uniform thin film has been fabricated on p-Si (100) substrate in a straightforward environment using spin coating technique. The authors of the present investigation believe that this study is one of the leading research for the preparation of a thin film using ZnO NPs. The essential properties such as structure and optical characteristics of the ZnO thin films fabricated on a p-Si (100) substrate were studied analytically through FESEM, XRD and FTIR spectrum. The FESEM analysis display that the ZnO/p-Si film in 2D developed through a spherical structure. Also, small and even grains of ZnO NPs are dispersed on the surface of the p-Si (100) wafer. XRD assessment indicated that the structure of ZnO on the substrate is pure crystalline with the zero oxygen flow. The remarks of IR absorbance spectra indicate that the ZnO thin film fabricated on p-Si (100) wafer possesses high crystalline quality. In a word, it is promising to produce extraordinary emission capability ZnO thin film on p-Si (100) wafer and it can be utilised as heterostructure and extending far down UV emission light-emitting diode apparatus.

**5. Acknowledgments:** Firstly, the authors direct their gratitude to the Soran research Centre, and Tishk International University for their facility and entrance fee to obtainable implements. Please contact the corresponding author for any further assistance regarding the experimental part in this investigation. This study was partially supported by Tishk International University (TIU) Research Center.

## 6 References

- [1] Hussain C.M.: 'Handbook of nanomaterials for industrial applications' (Elsevier Science, Cambridge, MA, USA, 2018)
- [2] Fanun M.: 'Colloids in biotechnology' (CRC Press, Boca Raton, FL, USA, 2010)
- [3] Kaviyarasu K., Maria Magdalane C., Kanimozhi K., *ET AL.*: 'Elucidation of photocatalysis, photoluminescence and antibacterial studies of ZnO thin films by spin coating method', *J. Photochem. Photobiol. B*, 2017, **173**, pp. 466–475
- [4] Jin X., Götz M., Wille S., *ET AL.*: 'A novel concept for self-reporting materials: stress sensitive photoluminescence in ZnO tetrapod filled elastomers', *Adv. Mater.*, 2013, **25**, (9), pp. 1342–1347
- [5] Lee J.-H.: Thin film transistor and method for preparing the same, 2015, Google Patents
- [6] Kumar V., Singh N., Kumar V., *ET AL.*: 'Doped zinc oxide window layers for dye sensitized solar cells', *J. Appl. Phys.*, 2013, **114**, (13), p. 134506
- [7] Ahn M.-W., Park K.-S., Heo J.-H., *ET AL.*: 'Gas sensing properties of defect-controlled ZnO-nanowire gas sensor', *Appl. Phys. Lett.*, 2008, **93**, (26), p. 263103
- [8] Alenezi M.R., Henley S.J., Silva S.: 'On-chip fabrication of high performance nanostructured ZnO UV detectors', *Sci. Rep.*, 2015, **5**, p. 8516

- [9] Xu T., Zhang L., Cheng H., *ET AL.*: 'Significantly enhanced photocatalytic performance of ZnO via graphene hybridization and the mechanism study'. *Appl. Catal., B*, 2011, **101**, (3-4), p. 382-387
- [10] Mirzaei H., Darroudi M.: 'Zinc oxide nanoparticles: biological synthesis and biomedical applications', *Ceram. Int.*, 2017, **43**, (1), pp. 907-914
- [11] Oh M.S., Lee K., Song J.H., *ET AL.*: 'Improving the gate stability of ZnO thin-film transistors with aluminum oxide dielectric layers', *J. Electrochem. Soc.*, 2008, **155**, (12), pp. H1009-H1014
- [12] Espitia P.J. P., Soares N.F.F., Coimbra J.S.R., *ET AL.*: 'Zinc oxide nanoparticles: synthesis, antimicrobial activity and food packaging applications', *Food Bioprocess. Technol.*, 2012, **5**, (5), pp. 1447-1464
- [13] Tankhiwale R., Bajpai S.: 'Preparation, characterization and antibacterial applications of ZnO-nanoparticles coated polyethylene films for food packaging', *Colloids Surf. B*, 2012, **90**, pp. 16-20
- [14] Girigoswami K., Viswanathan M., Murugesan R., *ET AL.*: 'Studies on polymer-coated zinc oxide nanoparticles: UV-blocking efficacy and in vivo toxicity', *Biointerphases*, 2015, **56**, pp. 501-510
- [15] Sirelkhatim A., Mahmud S., Seeni A., *ET AL.*: 'Review on zinc oxide nanoparticles: antibacterial activity and toxicity mechanism', *Nano-Micro Lett.*, 2015, **7**, (3), pp. 219-242
- [16] Agarwal H., Kumar S.V., Rajeshkumar S.: 'A review on green synthesis of zinc oxide nanoparticles – an eco-friendly approach', *Resour. Efficient Technol.*, 2017, **3**, (4), p. pp. 406-413
- [17] Buzeac C., Pacheco I.I., Robbie K.: 'Nanomaterials and nanoparticles: sources and toxicity', *Biointerphases*, 2007, **2**, (4), pp. MR17-MR71
- [18] Mohanpuria P., Rana N.K., Yadav S.K.: 'Biosynthesis of nanoparticles: technological concepts and future applications', *J. Nanopart. Res.*, 2008, **10**, (3), pp. 507-517
- [19] Al-Zoreky N.: 'Antimicrobial activity of pomegranate (*Punica granatum* L.) fruit peels', *Int. J. Food Microbiol.*, 2009, **134**, (3), pp. 244-248
- [20] Panth N., Manandhar B., Paudel K.R.: 'Anticancer activity of *Punica granatum* (pomegranate): a review', *Phytother. Res.*, 2017, **31**, (4), pp. 568-578
- [21] Cheng X.L., Zhao H., Huo L.H., *ET AL.*: 'ZnO nanoparticulate thin film: preparation, characterization and gas-sensing property', *Sens. Actuators B*, 2004, **102**, (2), pp. 248-252
- [22] Al-Hardan N.H., Jalar A., Hamid M.A., *ET AL.*: 'A wide-band UV photodiode based on n-ZnO/p-Si heterojunctions', *Sens. Actuators A*, 2014, **207**, pp. 61-66
- [23] Beek W.J., Wienk M.M., Janssen R.A.: 'Efficient hybrid solar cells from zinc oxide nanoparticles and a conjugated polymer', *Adv. Mater.*, 2004, **16**, (12), pp. 1009-1013
- [24] Adams R.M.C.: 'Land behind Baghdad: a history of settlement on the Diyala plains' (University of Chicago Press, Chicago, IL, USA, 1965)
- [25] Tyagi P.K., Tyagi S., Charul V., *ET AL.*: 'Estimation of toxic effects of chemically and biologically synthesized silver nanoparticles on human gut microflora containing *Bacillus subtilis*', *J. Toxicol. Environ. Health Sci.*, 2013, **5**, (9), pp. 172-177
- [26] Wei X.Q., Zhang Z.G., Liu M., *ET AL.*: 'Annealing effect on the microstructure and photoluminescence of ZnO thin films', *Mater. Chem. Phys.*, 2007, **101**, (2-3), pp. 285-290
- [27] Seeram N.P., *ET AL.*: 'Pomegranate phytochemicals, in pomegranates' (CRC Press, Boca Raton, FL, USA, 2006), pp. 21-48
- [28] Dadashi S., Mousazadeh M., Emam-Djomeh Z., *ET AL.*: 'Pomegranate (*Punica granatum* L.) seed: a comparative study on biochemical composition and oil physicochemical characteristics', *Int. J. Adv. Biol. Biomed. Res.*, 2013, **1**, (4), pp. 351-363
- [29] Nisha M.H., Tamileswari R., Jesurani S.: 'Analysis of anti-bacterial activity of silver nanoparticles from pomegranate (*Punica granatum*) seed and peel extracts', *Int. J. Eng. Res. Technol.*, 2015, **4**, (4), pp. 1044-1048
- [30] Jamdagni P., Khatri P., Rana J.S.: 'Green synthesis of zinc oxide nanoparticles using flower extract of *nyctanthes arbor-tristis* and their antifungal activity', *J. King Saud Univ., Sci.*, 2018, **30**, (2), pp. 168-175
- [31] Senthilkumar N., Nandhakumar E., Priya P., *ET AL.*: 'Synthesis of ZnO nanoparticles using leaf extract of *Tectona grandis* (L.) and their anti-bacterial, anti-arthritis, anti-oxidant and in vitro cytotoxicity activities', *New J. Chem.*, 2017, **41**, (18), pp. 10347-10356
- [32] Hinge S.P., Pandit A.B.: 'Solar-assisted synthesis of ZnO nanoparticles using lime juice: a green approach', *Adv. Nat. Sci., Nanosci. Nanotechnol.*, 2017, **8**, (4), p. 045006
- [33] Zak A.K., Abd. Majid W.H., Mahmoudian M.R., *ET AL.*: 'Starch-stabilized synthesis of ZnO nanopowders at low temperature and optical properties study', *Adv. Powder Technol.*, 2013, **24**, (3), pp. 618-624
- [34] Friedrich K., Breuer U.: 'Multifunctionality of polymer composites: challenges and new solutions' (William Andrew, Waltham, MA, USA, 2015)
- [35] Nirmla M., Anukaliani A.: 'Structural and optical properties of an undoped and Mn doped ZnO nanocrystalline thin film', *Photonics Lett. Poland*, 2010, **2**, (4), pp. 189-191
- [36] Singh R.P., Shukla V.K., Yadav R.S., *ET AL.*: 'Biological approach of zinc oxide nanoparticles formation and its characterization', *Adv. Mater. Lett.*, 2011, **2**, (4), pp. 313-317
- [37] Wu H., Zhao X., Li J., *ET AL.*: 'The large-area preparation and photoelectrochemical properties of graphene/ZnO nanorod composite film', *RSC Adv.*, 2017, **7**, (88), pp. 55673-55679
- [38] Hong R., Huang J., He H., *ET AL.*: 'Influence of different post-treatments on the structure and optical properties of zinc oxide thin films', *Appl. Surf. Sci.*, 2005, **242**, (3-4), pp. 346-352
- [39] Li Y.-Q., Fu S.-Y., Mai Y.-W.: 'Preparation and characterization of transparent ZnO/epoxy nanocomposites with high-UV shielding efficiency', *Polymer*, 2006, **47**, (6), pp. 2127-2132
- [40] Kaidashev E.M., Lorenz M., von Wenckstern H., *ET AL.*: 'High electron mobility of epitaxial ZnO thin films on c-plane sapphire grown by multistep pulsed-laser deposition', *Appl. Phys. Lett.*, 2003, **82**, (22), pp. 3901-3903
- [41] Zhang Y., Ram M.K., Stefanakos E.K., *ET AL.*: 'Synthesis, characterization, and applications of ZnO nanowires', *J. Nanomater.*, 2012, **2012**, p. 20
- [42] Wei X.Q., Huang J.Z., Zhang M.Y., *ET AL.*: 'Effects of substrate parameters on structure and optical properties of ZnO thin films fabricated by pulsed laser deposition', *Mater. Sci. Eng. B*, 2010, **166**, (2), pp. 141-146
- [43] Wei X., Zhao R., Shao M., *ET AL.*: 'Fabrication and properties of ZnO/GaN heterostructure nanocolumnar thin film on Si (111) substrate', *Nanoscale Res. Lett.*, 2013, **8**, (1), p. 112
- [44] Singh M., Sinha I., Mandal R.: 'Role of pH in the green synthesis of silver nanoparticles', *Mater. Lett.*, 2009, **63**, (3-4), pp. 425-427
- [45] Wang Y.-x., Jun Wen, Zhen Guo, *ET AL.*: 'Preparation of crystal oriented alpha-Sic films by pulsed ArF Laser deposition on Si (111)', *Chin. J. Semicond.*, 2000, **21**, (6), pp. 570-575
- [46] Sun Y., Miyasato T., Wigmore J.K.: 'Characterization of excess carbon in cubic Sic films by infrared absorption', *J. Appl. Phys.*, 1999, **85**, (6), pp. 3377-3379
- [47] Bagabas A., Alshammari A., About M.F.A., *ET AL.*: 'Room-temperature synthesis of zinc oxide nanoparticles in different media and their application in cyanide photodegradation', *Nanoscale Res. Lett.*, 2013, **8**, (1), p. 516